Large crystal local-field effects in second-harmonic generation of a Si/CaF_2 interface: An *ab initio* study

Matteo Bertocchi,[1,2] Eleonora Luppi,[3] Elena Degoli,[4] Valérie Véniard,[2] and Stefano Ossicini[4,5]
[1]*Dipartimento di Fisica, Università di Modena e Reggio Emilia, via Campi 213/A, 41125 Modena, Italy*
[2]*Laboratoire des Solides Irradiés, Ecole Polytechnique, Route de Saclay, F-91128 Palaiseau and European Theoretical Spectroscopy Facility (ETSF), France*
[3]*Department of Chemistry, University of California, Berkeley, California 94702, USA*
[4]*Istituto di Nanoscienze-CNR-S3 and Dipartimento di Scienze e Metodi dell'Ingegneria, Università di Modena e Reggio Emilia, Via Amendola 2 Padiglione Morselli, I-42122 Reggio Emilia, Italy*
[5]*Centro Interdipartimentale En&Tech, Via Amendola 2 Padiglione Morselli, I-42122 Reggio Emilia, Italy*
(Received 6 March 2012; published 11 July 2012)

In this work we present the *ab initio* study of crystal local-field effects in second-harmonic generation spectroscopy for an interface material such as Si/CaF_2. Starting from an independent particle picture, we demonstrate the fundamental importance of the polarization effects at the interface discontinuity. The estimation of the magnitude of crystal local-field effects for second-order nonlinear response in Si/CaF_2 interface was done by a comparative study with the absorption spectroscopy in the linear response. In both cases, we observe that the microscopic fluctuations due to the inhomogeneities of the system cause a decrease of the intensities of the spectra. However, for second-harmonic generation the decrease is selective and completely inhomogeneous while for absorption it is almost rigid. We also compare our theoretical study with experimental data showing unambiguously that only when crystal local fields are included, it is possible to correctly interpret experimental results.

DOI: 10.1103/PhysRevB.86.035309 PACS number(s): 78.67.De, 42.65.An, 71.15.Mb, 78.20.Bh

I. INTRODUCTION

Second-harmonic generation (SHG) is a nonlinear optical process which has been largely used for materials characterization.[1–6] It can give multiple information on the structural[7,8] and electronic properties of materials by detecting the modifications induced by the presence of adsorbates,[4] stress,[2] or external perturbing electromagnetic fields[9] and also permitting an *in situ* monitoring of dynamical processes.[4,5]

Sensitivity of SHG to the symmetry of the system is at the basis of all these different applications. Since SHG is dipole forbidden in centro-symmetric materials, a distinctive structural and electronic characterization of complex materials such as interfaces, surfaces, and nanostructures can be obtained from the signal originated by the symmetry-broken regions.[3,10]

In the last years different *ab initio* approaches that include many-body effects have been proposed.[11–17] However, their applications have been reserved to small bulk systems due to the huge computational effort required. Therefore, the theoretical investigations of nonlinear optical response of surfaces, superlattices, or interfaces[7,18,19] have usually been performed at the level of the independent particle approximation (IPA) considering a scissor operator (SO)[2,20] or GW corrections.[21] Instead, studies on these complex systems that include many-body effects such as excitons and crystal local fields (LFs) are usually restricted to phenomenological,[22] semiempirical,[23] or classical models.[24,25] However, these many-body effects are expected to give important contributions to the SHG signal. In fact, there are many experimental evidences about the strong modifications on the second-order nonlinear optical response due to the microscopic environment.[5,26] Crystal local fields are generated by the induced microscopic response of the system by an external perturbation. As a consequence, their effects will be particularly important close to discontinuity regions as in interface materials.

In this work we present an *ab initio* study of crystal local-field effects in SHG spectroscopy for the Si/CaF_2 interface.[1] Going beyond an independent particle picture, we explicitly include in second-order response the contribution from the induced local electric field at the discontinuity region between Si (semiconductor) and CaF_2 (insulator) slabs. In fact, as these slabs are both centro-symmetric, the SHG signal is only generated by breaking the symmetry at the insulator-semiconductor interface. We also compare our theoretical results with experiments.[1] This also permits us to confirm the experimental analysis concerning the nature of this interface with respect to the growth conditions.[27,28]

In this contest, Si/CaF_2 interface is a highly suited material to study because of its optical and electronic properties. Indeed, it is possible to nanostructure Si and CaF_2 by superimposing semiconducting and insulating slabs in a multiquantum well. This consents to exploit the relation between optical properties and quantum confinement effects of Si[29–31] where CaF_2 plays the role of excellent insulator. In fact, CaF_2 energy gap is of 12 eV which makes this material transparent in a wide frequency range. In particular, the optical properties in the low-energy region have been observed to strongly depend on the interface electronic states.[31] Therefore, a great effort has been done in order to understand the possible geometrical configuration that determines these states[32–34] and its dependency on the growth conditions.[27,28] Besides the linear optical properties, the Si/CaF_2 interface has also important nonlinear optical properties which have been investigated experimentally by Heinz *et al.*[1] They used optical second harmonic to probe the electronic transitions in order to understand the distinctive nature of the interfacial region. We used this experimental work for comparison with our calculated SHG spectra.

II. FORMALISM

The quantity that is experimentally measured is the absolute value of the macroscopic second-order susceptibility $\chi_M^{(2)}$ which is defined as $\mathbf{P}_M^{(2)} = \chi_M^{(2)}\mathbf{E}_{\mathrm{TOT}}\mathbf{E}_{\mathrm{TOT}}$ where $\mathbf{P}_M^{(2)}$ is the macroscopic second-order polarization and $\mathbf{E}_{\mathrm{TOT}}$ is the macroscopic component of the total electric field. The quantity $\mathbf{E}_{\mathrm{TOT}}$ contains both the external perturbing field and the induced field as generated by the perturbation. The latter comprehends the microscopic fluctuations due to the nonhomogeneities of the studied system. These give rise to an additional microscopic field that affects the whole response of the system and which is responsible for the crystal local-field effects.

We have studied SHG spectroscopy evaluating the effects of the crystal local fields on the macroscopic second-order response function by using the *ab initio* formalism recently presented in Refs. 15 and 16 which is based on the time-dependent density-functional theory (TDDFT). Within this theoretical derivation it is possible to calculate the frequency-dependent second-order susceptibility $\chi^{(2)}$ explicitly including crystal local-field and excitonic effects. In the presented calculations only crystal local fields have been considered as variations in the Hartree potential related to the local induced fields. Excitonic effects demonstrated to be very small in the investigated system and their contribution have been neglected. This is not in contrast with the previous results of Refs. 15 and 16 but underlines how the different physical nature of the systems determines the relative importance of these two effects. In the present case the interface is responsible for the SHG signal, making predominant the sharp variation of the potential in the interface region (i.e., the local fields), with respect to other many-body effects.

To compare with experiments we have calculated $|\chi_{zzz}^{(2)}|$ which corresponds to light polarized along the **z** direction (i.e., perpendicular to the interface[1]). In our formalism[15] it is related to the second-order response functions $\chi_{\rho\rho\rho}^{(2)}$ as follows:

$$\chi_{zzz}^{(2)} = \frac{-i}{4}\epsilon_M(\mathbf{z},2\omega)\epsilon_M(\mathbf{z},\omega)\epsilon_M(\mathbf{z},\omega)\chi_{\rho\rho\rho}^{(2)}(2\mathbf{z},\mathbf{z},\mathbf{z},\omega,\omega), \quad (1)$$

where ϵ_M is the macroscopic dielectric function. Its relation to the microscopic dielectric function ϵ is[35]

$$\epsilon_M(\hat{\mathbf{q}},\omega) = \lim_{q\to 0}\frac{1}{\epsilon^{-1}_{\mathbf{G}=\mathbf{0},\mathbf{G}'=\mathbf{0}}(\mathbf{q},\omega)}, \quad (2)$$

where $\mathbf{q}$ represents the light polarization vectors while $\mathbf{G}$ are the reciprocal lattice vectors. The inverse dielectric tensor $\epsilon^{-1}_{\mathbf{G},\mathbf{G}'}$ is directly related to the first-order response $\chi_{\rho\rho}^{(1)}$ through the Coulomb potential u as follows:

$$\epsilon^{-1}_{\mathbf{G},\mathbf{G}'}(\mathbf{q},\omega) = 1 + u(\mathbf{q}+\mathbf{G})\chi^{(\mathbf{1})}_{\rho\rho\mathbf{G},\mathbf{G}'}(\mathbf{q},\omega). \quad (3)$$

The response functions $\chi_{\rho\rho}^{(1)}$ and $\chi_{\rho\rho\rho}^{(2)}$ are obtained in TDDFT through the Dyson-like equations:[16]

$$\left[1 - \chi_0^{(1)}(\omega)f_u(\omega)\right]\chi_{\rho\rho}^{(1)}(\omega) = \chi_0^{(1)}(\omega), \quad (4)$$

$$\left[1 - \chi_0^{(1)}(2\omega)f_u(2\omega)\right]\chi_{\rho\rho\rho}^{(2)}(2\omega,\omega) = \chi_0^{(2)}(2\omega,\omega)\left[1 + f_u(\omega)\chi_{\rho\rho}^{(1)}(\omega)\right]\left[1 + f_u(\omega)\chi_{\rho\rho}^{(1)}(\omega)\right], \quad (5)$$

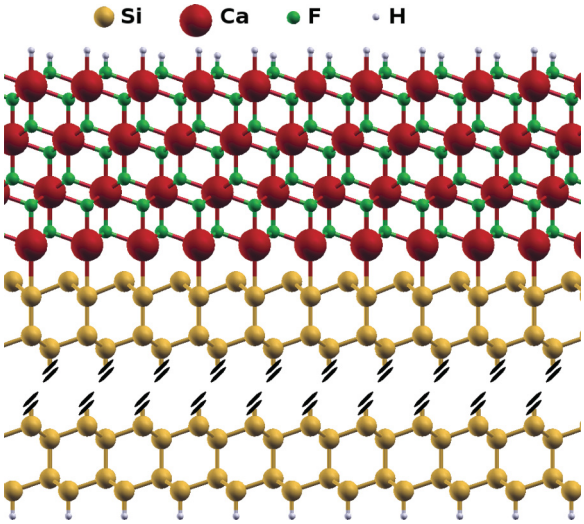

FIG. 1. (Color online) T_4 interface structure. Ca atoms (red) are on top of the second layer Si atoms (yellow) while F (green) atoms do not bond to Si. The surfaces are passivated with H atoms (white). Only the four outermost Si double layers are shown.

where $\chi_0^{(1)}$ and $\chi_0^{(2)}$ represent the first- and second-order response functions in IPA while f_u kernel is given by the Hartree potential $f_u = \frac{\delta V_H}{\delta\rho} = u$ and it is responsible for the crystal local fields. We finally would like to note that we have omitted the explicit dependence on the **q** and **G** vectors in Eqs. (4) and (5) for a better comprehension of the formalism.

III. RESULTS

We computed SHG spectroscopy on the Si(111)/CaF_2 interface in a T_4 configuration with B-type orientation[28,34] along the **z** direction as shown in Fig. 1. In this particular configuration Ca atoms at the interface are in T_4 high symmetry sites while F atoms at the interface are in H_3 sites. The choice of this configuration comes from the match between the sample synthesis conditions (700 °C) described by Heinz[1] and the latest studies on the effects of growth parameters on the structural interface features.[27,28]

We studied the T_4 B-type configuration of Si/CaF_2 in density-functional theory (DFT) within local-density approximation (LDA) using the plane-wave pseudopotential method[16] and the supercell technique implemented in the ABINIT package.[36] We obtained for the relaxed cell parameters, respectively, $a_{CaF_2} = 5.410$ Å and $a_{Si} = 5.389$ Å with a lattice mismatch of 0.4%. These theoretical values calculated at 0 K well reproduce the experimental values $a_{CaF_2} = 5.447$ Å and $a_{Si} = 5.430$ Å at 6.4 K.[37]

To reproduce the bulk features in the near-interface regions we used a thickness of 44.3 Å for Si slab and of 12.2 Å for CaF_2 slab. We have also relaxed the in-plane lattice parameter of the interface to diminish the stress caused by the lattice mismatch. The large thickness of Si compared to CaF_2 is due to the crucial role that Si electronic states play at the band edges because of the quite different energy gaps of these materials. Finally, in order to create a single interface structure we included about 30 Å of vacuum into the simulation cell and passivated both the external surfaces with hydrogen atoms.

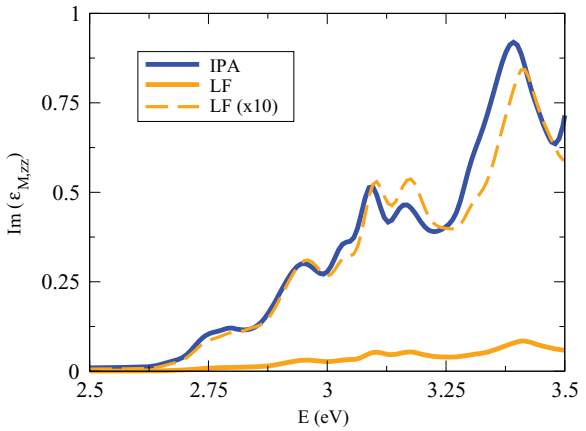

FIG. 2. (Color online) Absorption spectra [Im($\epsilon_{M,zz}$)] in the **z** direction calculated in IPA (blue/dark-gray continuous line) and with inclusion of LF effects (orange/light-gray continuous line). For a clearer comparison the LF curve has been multiplied by a factor of 10 (orange/light-gray dashed line).

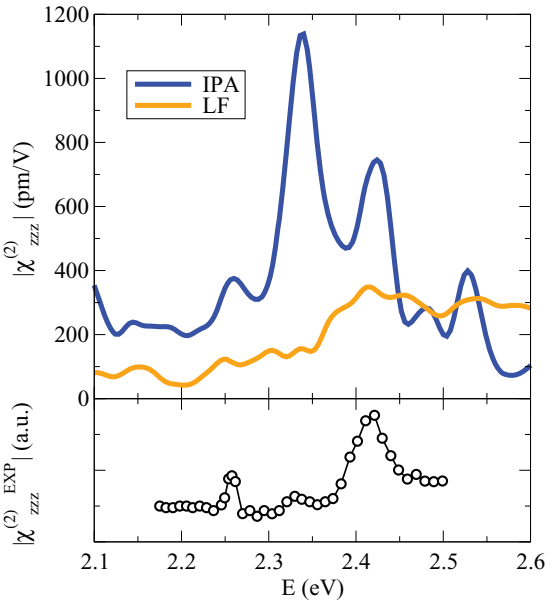

FIG. 3. (Color online) Second-harmonics generation spectra ($\chi^{(2)}_{zzz}$) calculated in IPA (blue/dark-gray line) and including LFs (orange/light-gray line). The experimental SHG spectrum from Ref. 1 is also reported (black line and circles) on the lower part of the graphic.

Starting from the optimized interface structure we computed $\chi^{(2)}_{zzz}$ as in Eq. (1) using the 2LIGHT code[16] where our nonlinear TDDFT formalism is implemented.[38] We observe that, in our approach, the effects of the crystal local fields enter through ϵ_M of Eq. (2) and through $\chi^{(2)}_{\rho\rho\rho}$ obtained from the second-order Dyson equation [Eq. (5)]. So in order to estimate the magnitude of these effects we have performed a comparative study with the linear absorption spectroscopy which is the imaginary part of ϵ_M [Eq. (2)].

To compare our theoretical SHG spectrum with the experimental one[1] we have applied a scissor operator (SO) correction of 1.07 eV to the LDA energy gap in order to match the measured value of 2.4 eV at Γ.

The linear optical-absorption spectra for light polarized along the **z** direction are shown in Fig. 2. We observe that in this energy region the presence of the LF strongly influences the linear optical properties of the system, the whole intensity is lowered by about 10 times with respect to the independent particle response. However, the main features of the spectrum like the position of the peaks, the shape, and the relative intensities are only slightly modified. We have verified that this drastic reduction is characteristic of the discontinuous direction z and negligible for the other more homogeneous components $\epsilon_{M,xx}$ and $\epsilon_{M,yy}$. Similar decrease in the low-energy region due to the strong polarization effects at the interface has been observed also in other Si-based systems like nanocrystals[39] and surfaces.[40] It is important to point out that unlike in the nonlinear optics here both the interface and the bulk contribute to the total signal.

In Fig. 3 we report the calculated SHG spectra together with experimental data.[1] The experimental spectrum [see Fig. 1(a) of Ref. 1], originally in arbitrary units, has been reproduced for an easy comparison with our theoretical results. In the IPA response the energy position of the three main experimental peaks (2.26, 2.33, and 2.42 eV) are recovered but their relative intensities are wrong. In particular, the intensity of the second peak is strongly overestimated. When LFs are included the energy position of the peaks remains practically unchanged while their height is in general diminished in this low-energy region of the spectrum. The same trend has been observed for SiC and GaAs bulk semiconductors.[16] Nevertheless, with respect to these homogeneous systems, for Si/CaF_2 the SHG reduction and hence its dependence on LF effects is more important because of the discontinuity region. This behavior (i.e., the significant influence of LFs on the spectrum) also occurs in the linear optic outcomes but with some noticeable differences. In fact, while IPA and LF absorption spectra almost coincide, apart from a constant factor (Fig. 2), IPA and LF SHG spectra present a different intensity modulation for each peak. This is the consequence of the specific local environment that surrounds the interface discontinuity where the SHG process is generated. In particular, in IPA the SHG peak at 2.33 eV seems to be the most important feature in the spectrum while with the inclusion of the LF this peak is instead drastically diminished with respect to the others. We also note that the peaks at 2.26 and 2.42 eV substantially keep their relative intensity with the inclusion of the LF which also contributes to flatten out the peaked structure above 2.5 eV. Once we compare with the experiment it is evident that only including the LF effects one can obtain a good agreement in terms of both energy positions and relative intensity of the peak structures. According to Eq. (1) we can notice that while the dielectric function is diminished by one order of magnitude (Fig. 2), $\chi^{(2)}_{\rho\rho\rho}$ should be considerably increased to compensate its effects, recovering almost the same $\chi^{(2)}_{zzz}$ intensity of the IPA result (Fig. 3). Additionally, all the information about the modifications of the SHG curve are mostly contained in $\chi^{(2)}_{\rho\rho\rho}$, since the form of ϵ_M is almost unchanged and variations are small and slow with respect to the SHG range. This highlights how, for inhomogeneous systems where the potential undergoes rapid variations, the second-order density response functions $\chi^{(2)}_{\rho\rho\rho}$ become the key quantity for the SHG

process and LF effects become predominant on the studied system. Moreover, such a significant agreement confirms the experimental investigations[27,28] that attribute a T_4 B-type nature to the Si/CaF_2 interface grown at temperature above 700 °C.

IV. CONCLUSIONS

In conclusion, we have shown that an independent particle picture can give a qualitative description of the SHG process in the Si/CaF_2 interface, recovering the main features (in terms of energy peak position) originated from the anisotropies of the system. However, to match the spectral line shape of the experiment, LF effects become essential. In fact, LFs strongly influence the second-order nonlinear response close to the discontinuity region inducing a significant redistribution of the intensity. We demonstrated that this redistribution is largely more dramatic in nonlinear optical response than in the linear response. For SHG the lowering of the intensities is selective and not homogeneous while for absorption the shape of the spectrum is almost unchanged. Our results have far-reaching consequences beyond the specific interface we have studied. The microscopic induced polarization can have large and unpredictable effects on the SHG process becoming essential for complex systems.

ACKNOWLEDGMENTS

This work has been performed under the HPC-EUROPA2 project (Project No. 228398) with the support of the European Commission–Capacities Area–Research Infrastructures. We also acknowledge CINECA CPU time granted by ISCRA C projects and financial support from Camera di Commercio di Reggio Emilia project "Internazionalizzazione di Qualità."

[1] T. F. Heinz, F. J. Himpsel, E. Palange, and E. Burstein, Phys. Rev. Lett. **63**, 644 (1989).
[2] M. Cazzanelli, F. Bianco, E. Borga, G. Pucker, M. Ghulinyan, E. Degoli, E. Luppi, V. Véniard, S. Ossicini, D. Modotto, S. Wabnitz, R. Pierobon, and L. Pavesi, Nat. Mater. **11**, 148 (2012).
[3] G. Lüpke, Surf. Sci. Rep. **35**, 75 (1999).
[4] U. Höfer, Appl. Phys. A **63**, 533 (1996).
[5] W. A. Tisdale, K. J. Williams, B. A. Timp, D. J. Norris, E. S. Aydil, and X.-Y. Zhu, Science **328**, 1543 (2010).
[6] D. Hsieh, J. W. McIver, D. H. Torchinsky, D. R. Gardner, Y. S. Lee, and N. Gedik, Phys. Rev. Lett. **106**, 057401 (2011).
[7] V. I. Gavrilenko, Phys. Rev. B **77**, 155311 (2008).
[8] J. R. Power, J. D. O'Mahony, S. Chandola, and J. F. McGilp, Phys. Rev. Lett. **75**, 1138 (1995).
[9] M. W. Klein, C. Enkrich, M. Wegener, and S. Linden, Science **313**, 502 (2006).
[10] Y. R. Shen, *The Principles of Nonlinear Optics* (Wiley-Interscience, New York, 1984).
[11] Z. H. Levine and D. C. Allan, Phys. Rev. Lett. **66**, 41 (1991).
[12] A. Dal Corso, F. Mauri, and A. Rubio, Phys. Rev. B **53**, 15638 (1996).
[13] E. K. Chang, E. L. Shirley, and Z. H. Levine, Phys. Rev. B **65**, 035205 (2001).
[14] R. Leitsmann, W. G. Schmidt, P. H. Hahn, and F. Bechstedt, Phys. Rev. B **71**, 195209 (2005).
[15] E. Luppi, H. Hübener, and V. Véniard, J. Chem. Phys. **132**, 241104 (2010).
[16] E. Luppi, H. Hübener, and V. Véniard, Phys. Rev. B **82**, 235201 (2010).
[17] H. Hübener, E. Luppi, and V. Véniard, Phys. Rev. B **83**, 115205 (2011).
[18] J. E. Mejía, B. S. Mendoza, M. Palummo, G. Onida, R. Del Sole, S. Bergfeld, and W. Daum, Phys. Rev. B **66**, 195329 (2002).
[19] S. Sharma, J. K. Dewhurst, and C. Ambrosch-Draxl, Phys. Rev. B **67**, 165332 (2003).
[20] J. L. Cabellos, B. S. Mendoza, M. A. Escobar, F. Nastos, and J. E. Sipe, Phys. Rev. B **80**, 155205 (2009).
[21] B. Adolph and F. Bechstedt, Phys. Rev. B **62**, 1706 (2000).
[22] S. A. Yang, X. Li, A. D. Bristow, and J. E. Sipe, Phys. Rev. B **80**, 165306 (2009).
[23] J. Mejía, B. S. Mendoza, and K. Pedersen, Surf. Sci. **605**, 941 (2011).
[24] Y. Zeng, W. Hoyer, J. Liu, S. W. Koch, and J. V. Moloney, Phys. Rev. B **79**, 235109 (2009).
[25] E. J. Adles and D. E. Aspnes, Phys. Rev. B **77**, 165102 (2008).
[26] M. I. Stockman, D. J. Bergman, C. Anceau, S. Brasselet, and J. Zyss, Phys. Rev. Lett. **92**, 057402 (2004).
[27] C. A. Lucas, D. Loretto, and G. C. L. Wong, Phys. Rev. B **50**, 14340 (1994).
[28] J. Harada *et al.*, J. Cryst. Growth **163**, 31 (1996).
[29] S. Ossicini, A. Fasolino, and F. Bernardini, Phys. Rev. Lett. **72**, 1044 (1994).
[30] F. Bassani, I. Mihalcescu, J. C. Vial, and F. A. d'Avitaya, Appl. Surf. Sci. **117-118**, 670 (1997).
[31] E. Degoli and S. Ossicini, Phys. Rev. B **57**, 14776 (1998).
[32] J. Zegenhagen and J. R. Patel, Phys. Rev. B **41**, 5315 (1990).
[33] S. Ossicini, C. Arcangeli, and O. Bisi, Phys. Rev. B **43**, 9823 (1991).
[34] H. Fujitani and S. Asano, Surf. Sci. **268**, 265 (1992).
[35] S. L. Adler, Phys. Rev. **126**, 413 (1962).
[36] X. Gonze *et al.*, Computer Phys. Commun. **180**, 2582 (2009); Zeit. Kristallogr. **220**, 558 (2005).
[37] D. N. Batchelder and R. O. Simmons, J. Chem. Phys. **41**, 2324 (1964).
[38] We used 5000 plane waves, 130 bands, $G^{\text{cut}} = 9$ and 608 random K points to converge optical spectra. A Gaussian broadening of 0.013 eV has also been applied.
[39] R. Guerra, M. Marsili, O. Pulci, and S. Ossicini, Phys. Rev. B **84**, 075342 (2011).
[40] L. Caramella, G. Onida, F. Finocchi, L. Reining, and F. Sottile, Phys. Rev. B **75**, 205405 (2007).